Ultrastructural and morphometric effect of aluminum phosphate and calcium phosphate nanoparticles as adjuvants in vaccinated mice

Mohamed S. Salim[a], Aliaa M. Issa[b], Abdel Razik H. Farrag[c], Hamdalla H. Zidan[d], Aly F. Mohamed[a]

[a]Holding Company for Biological Products and Vaccines (VACSERA), Giza, [b]Department of Zoology, Faculty of Science, Giza, [c]Department of Pathology, National Research Center, Cairo, [d]Department of Microbiology and Immunology, Faculty of Pharmacy, Cairo University, Cairo, Egypt

Correspondence to Abdel Razik H. Farrag, PhD, Department of Pathology, Medical Division Research, National Research Center, Cairo 12622, Dokki, Egypt Tel. +011 1127 1760;. e-mail: abdelrazik2000@yahoo.com

Received 24 March 2016
Accepted 19 May 2016

Journal of The Arab Society for Medical Research 2016, 11:22–28

Background/aim
Calcium phosphate (CAP) and aluminum phosphate (alum) compounds have been approved as vaccine adjuvants for humans. The present study aimed to study the ultrastructural and morphometric effect of both aluminum phosphate (alum) and CAP nanoparticle adjuvant.
Materials and methods
Eighteen Swiss albino mice were used in the experiment. An overall 50% of them were adult and the other 50% were juvenile. Mice were immunized intramuscularly with 0.125 ml of adjuvanted tetanus toxoid vaccine. In the alum adjuvant group, three adult mice and another three juvenile ones were injected with alum adjuvanted vaccine and killed 1 week after immunization. In the CAP adjuvant group, three adult mice and another three juvenile mice were injected with CAP adjuvanted vaccine and killed 1 week after immunization. At the end of the work, samples of the liver, kidney, and brain were subjected to light and electron microscopic examinations.
Results
In both the alum group and the CAP nanoparticle adjuvant group, the examination revealed wide and severe ultrastructural changes in the liver, kidney, and brain of adult and juvenile mice. These changes included swollen mitochondria with degenerated cristae, severely degenerated ground cytoplasm, and unusual chromatin picture of nucleus. In contrast, morphometric studies of the nucleus/cell ratio and damaged areas showed a significant increase in the liver, kidney, and brain of both adjuvants.
Conclusion
The results of this study revealed that both aluminum phosphate (alum) and CAP nanoparticle adjuvant caused ultrastructural and morphometric changes in tissues of the liver, kidney, and brain.

Keywords:
aluminum phosphate, calcium phosphate vaccinated mice, morphometric, ultrastructural

J Arab Soc Med Res 11:22–28

1687-4293

Introduction

Since the earliest attempts to raise significant immune responses against nonliving agents, investigators have tried to identify useful additives that can be combined with antigens to enhance immune responses. Such immune-enhancing additives are known as *adjuvants*. The term 'adjuvant' (from the latin, adjuvare=help) was first coined by Ramon in 1926 [1]. Virtually, all adjuvant systems developed, to date, have focused on one of the two mechanisms: specific immune activation or the delivery depot effect [2]. Although many adjuvant systems have been developed and tested in preclinical models, few have actually proved useful for human vaccines. Manmohan [2] stated that the primary limitations for the use of new adjuvant systems with human vaccines revolve around safety issues. However, the toxicity of adjuvants has been reduced systematically through research and development efforts over the last 80 years, and the safety barriers presented by regulatory and liability issues have continued to increase [2]. In the USA, alum compounds are the most extensively used adjuvants in licensed vaccines for humans [2]. Although they effectively enhance immune responses, there are several disadvantages associated with their use [3]. The disadvantages of alum-based adjuvants include the severity of local tissue irritation, the longer duration of the inflammatory reaction at the injection site, minimal induction of cell-mediated immunity, and a propensity to elicit undesirable immunoglobulin E responses [4–6]. For these

reasons, new adjuvants are being developed to enhance the immunity against weak antigens. Nanomaterials have unique physicochemical properties, such as ultra small size, large surface area-to-mass ratio, and high reactivity, which are different from bulk materials of the same composition. These properties can be used to overcome some of the limitations found in traditional vaccines [7]. Efforts with calcium adjuvants have continued, and work with calcium phosphate (CAP) nanoparticles has had some preclinical success [8]. CAP and aluminum phosphate (alum) compounds have been approved as vaccine adjuvants for human use in several European countries [9]. Therefore, the study aimed to evaluate the pathological, ultrastructural, and morphometrical effects of both aluminum phosphate and CAP nanoparticle adjuvants.

Materials and methods

Animals

Eighteen Swiss albino mice obtained from the Egyptian Company for the Production of Sera and Vaccines (EgyVac.), affiliate of the Holding Company for Biological Products and Vaccines (VACSERA), were used in the experiment. Nine of them were adult (18–22 g) and the other nine were juvenile (10–12 g). The mice were housed under standard conditions in plastic laboratory cages in the animal facility of the same place. The animals were divided into groups and immunized as shown in the experimental design.

Experimental design

In this study, 18 Swiss albino mice were used. The mice were obtained from the Egyptian Company for the Production of Sera and Vaccines (EgyVac.), affiliate of the Holding Company for Biological Products and Vaccines (VACSERA). Nine of them were adult (18–22 g) and the other nine were juvenile (10–12 g). The animals were housed under standard conditions in plastic laboratory cages in the animal facility of the same place. The mice were divided into main three groups as follows: the control group, the alum adjuvant group, and the CAP group. In each group, three adult mice were killed at first week after immunization and three juvenile mice were killed at first week after immunization.

Preparation of adjuvant

Aluminum phosphate (alum) adjuvant

Both 0.63 mol/l $AlCl_3 0.6H_2O$ and 0.3 mol/l $Na_3PO_4 0.12H_2O$ were individually dissolved in 40 ml distilled water. The prepared solutions were filtered using a 0.2 μm filter. The contents were stirred continuously during the procedure at 40–60 rpm. The 0.3 mol/l $Na_3PO_4 0.12H_2O$ solution was added to a mixing bottle. Thereafter, 300 ml sterile distilled water was added. Tetanus toxoid was added followed by the addition of 0.63 mol/l $AlCl_3 0.6H_2O$ solution to the mixing bottle. The pH was maintained between 6.5 and 6.8. The final volume was adjusted with sterile distilled water. The suspension was mixed for 2 h at 37°C [10,11].

Calcium phosphate nanoparticle adjuvant

CAP nanoparticle adjuvant was prepared by mixing solution A and solution B. Solution A was prepared by means of rapid dissolution of 18.36 g of $Na_2HPO_4 12H_2O$, 12.5 g of NaOH, and 7.5 g of $NaHCO_3$ in 325 ml of distilled water. Solution B was prepared by means of rapid dissolution of 10.75 g of $Ca(NO_3)2.4H_2O$ in 125 ml of distilled water. All solutions were sterilized by means of membrane filtration (0.022 Stereoscopy vacuum filtration system; Millipore, Temecula, California, USA). Tetanus toxoid was homogenized in 0.07 mol/l dibasic sodium phosphate sterile solution. The vaccine suspension was mixed with solution A before solution B. The precipitate of gel-like amorphous CAP formed was agitated for ~30 s [10].

Electron microscopic examination

The examination was carried out at the first week after immunization. The specimens were prepared according to the procedure described by Anderson and Cheville [12], Anderson *et al.*[13], and Coulter [14].

Morphometric examination

This examination was carried out on the liver, kidney, and brain 1 week after immunization on all groups. The data were obtained using the Leica Qwin 500 Image Analyzer computer system (Cambridge, England). The image analyzer consisted of a colored video camera, colored monitor, and a hard disc of IBM personal computer connected to the microscope, and was controlled by Leica Qwin 500 software [15].

Statistical analysis

Statistical calculations were carried out with the SPSS 10.0 for Windows software package (Statistica, San Jose, California, USA). The results were expressed as mean ± SE. Analysis of variance and Student's *t*-test were used for statistical analyses; *P* values less than 0.05 were considered significant [15].

Results

Electron microscopic study

Effect on the liver

Electron microscopic examination of liver tissue of control nonimmunized mice showed similar normal

structure in both adult and juvenile mice, which includes normal cellular organelles such as nucleus, Golgi apparatus, mitochondria, and rough endoplasmic reticulum (Fig. 1a).

In the alum groups, wide and severe ultrastructural changes were observed. The liver tissue of adult mice showed unusual chromatin picture of nucleus, degenerative nuclear envelope, and most of the ground cytoplasm was moderately degenerated (Fig. 1b). The liver of juvenile mice showed nucleus with unusual chromatin picture, degenerated nuclear envelope, vacuolated and moderately degenerated cytoplasm, and swollen mitochondria associated with degenerated cristae (Fig. 1c).

When using CAP nanoparticle adjuvants, the change in ultrastructures of adult mice included swollen mitochondria with degenerated cristae and reduction in the number of chromosomes on rough endoplasmic reticulum, whereas the changes in juvenile mice included huge amount of lysosomes and swollen mitochondria (Fig. 1d and e).

Effect on the kidney

Electron microscopic examination of kidney tissue of control nonimmunized mice showed similar normal structure in both adult and juvenile mice: normal cellular organelles such as nuclei, which lie almost at the center of the cell, and rough endoplasmic reticulum with the infolding of the basal membrane (Fig. 2a).

The ultrastructural changes occurring in the kidney of both adult and juvenile mice in the alum adjuvant group included developing large vacuoles containing cell debris, shrunken nuclei with irregular outline, unusual chromatin picture of nucleus, and appearance of lymphocytes (Fig. 2b and c).

In the CAP nanoparticle adjuvant group, the changes included swollen mitochondria with degenerated

Figure 1

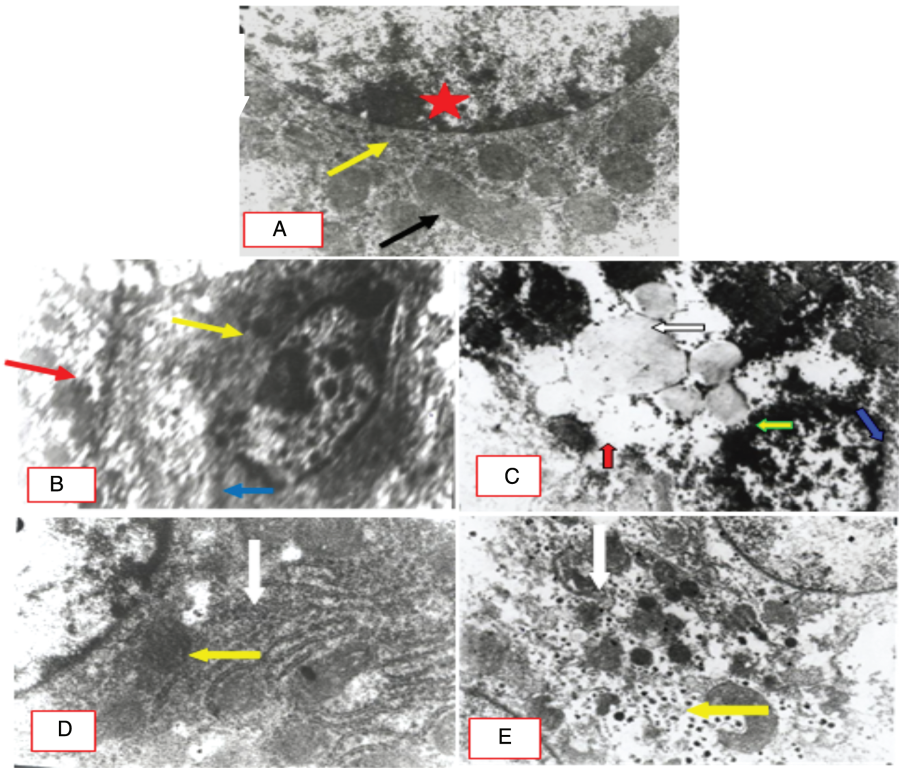

Electron micrograph of liver sections: (a) a control nonimmunized mouse shows normal structure of nucleus (star), mitochondria (black arrow), and Golgi apparatus (yellow arrow) (×15 000); (b) an adult mouse immunized with tetanus toxoid adsorbed on alum adjuvant 1 week after immunization shows nucleus displaying unusual chromatin picture (yellow arrow) and degenerative nuclear envelope (blue arrow). Most of the ground cytoplasm is moderately degenerated (red arrows) (×8000); (c) a juvenile mouse immunized with tetanus toxoid adsorbed on alum adjuvant 1 week after immunization shows nucleus with unusual chromatin picture (yellow arrow), degenerated nuclear envelope (blue arrow), vacuolated and moderately degenerated cytoplasm (red arrows), and swollen mitochondria associated with degenerated cristae (white arrow) (×8000); (d) an adult mouse immunized with tetanus toxoid adsorbed on calcium phosphate nanoparticle adjuvant 1 week after immunization shows few ribosomes on the rough endoplasmic reticulum (white arrows) and swollen mitochondria associated with degenerative cristae were noticed (yellow arrow) (×8000); (e) a juvenile mouse immunized with tetanus toxoid adsorbed on calcium phosphate nanoparticle adjuvant 1 week after immunization shows huge amount of lysosome (white arrows) and degenerated or swollen mitochondria (yellow arrow) (×8000).

Figure 2

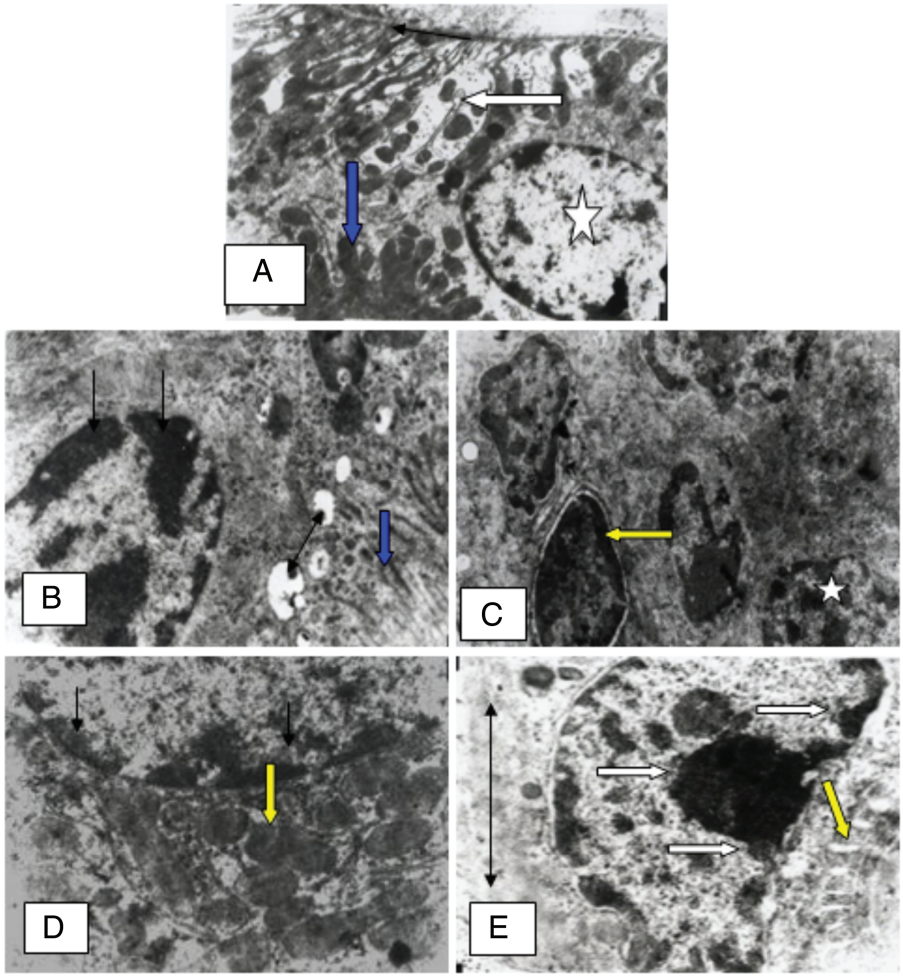

Electron micrograph of kidney sections: (a) a control nonimmunized mouse showing the enfolding of the basal membrane (blue arrow), rough endoplasmic reticulum (white arrow), few numbers of microvilli (blue arrow), and the nucleus (star) (×8000); (b) an adult mouse immunized with tetanus toxoid adsorbed on alum adjuvant 1 week after immunization showing a part of a proximal convoluted tubule (blue arrow). Notice the developed large vacuoles (double head arrow) containing cell debris and usually associated with mitochondria; the nucleus appeared with irregular outline and associated with condensed chromatin (black arrows) (×8000); (c) a juvenile mouse immunized with tetanus toxoid adsorbed on alum adjuvant 1 week after immunization shows the appearance of lymphocytes (yellow arrow). Notice that most of the mitochondria exhibited degenerated cristae, severely degenerated ground cytoplasm, and the nucleus with unusual chromatin picture (yellow arrow) (×8000); (d) a mouse immunized with tetanus toxoid adsorbed on calcium phosphate nanoparticle adjuvant 1 week after immunization shows most of the mitochondria exhibiting degenerated cristae or swollen (yellow arrow) and the nucleus displayed unusual chromatin picture (black arrows) (×8000); (e) a juvenile mouse immunized with tetanus toxoid adsorbed on calcium phosphate nanoparticle adjuvant 1 week after immunization shows that most of the mitochondria exhibited degeneration (yellow arrow), the ground cytoplasm is severely degenerated (double head arrow), and the nucleus displayed unusual chromatin picture (white arrows) (×15 000).

cristae, severely degenerated ground cytoplasm, and unusual chromatin picture of nucleus (Fig. 2d and e).

Effect on the brain

Electron microscopic examination of brain tissue of control nonimmunized mice showed similar normal structure in both adult and juvenile mice. The cytoplasm contained many mitochondria; the nucleus showed regular chromatin structure, and the supporting cells had large nucleus and small cytoplasm that include few organelles (Fig. 3a).

The ultrastructural changes occurring in the brain of adult mice included appearance of vacuoles containing fine granular and dense material and intact cell organelles; however, the juvenile mice showed appearance of few dense bodies and many shrunken mitochondria, whereas other organelles appeared intact in the lower part of the cell (Fig. 3b and c).

In the CAP nanoparticle adjuvant group, the ultrastructural changes in the adult and the juvenile group were similar and included the appearance of necrotic tissue surrounding the upper and lower border of the cell and some vacuoles containing dense bodies, whereas others contained pale bodies (Fig. 3d and e).

Figure 3

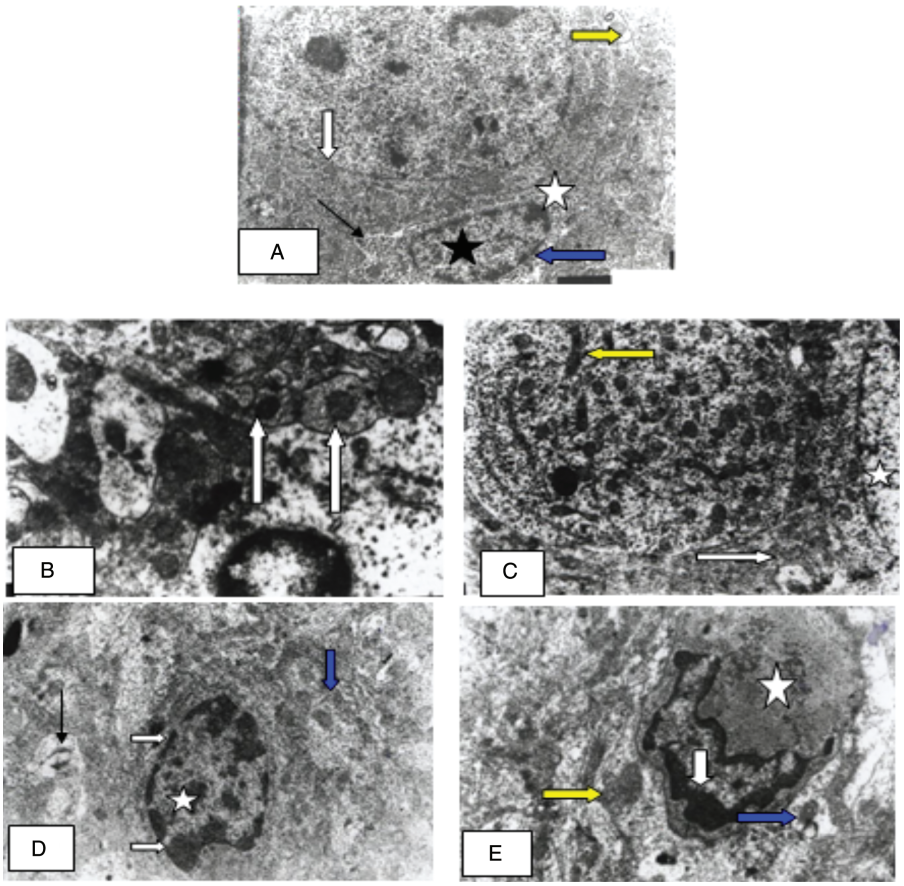

Electron micrograph of brain sections: (a) a control nonimmunized mouse shows a part of a neuron of the cerebral cortex. The cytoplasm contains many mitochondria (yellow arrow) and a large nucleus (white star) with regular chromatin structure (white arrow). Notice the supporting cell (blue arrow) at the lower with large nucleus (black star) and cytoplasm (black arrow) that include few organelles (×10 000); (b): an adult mouse immunized with tetanus toxoid adsorbed on alum adjuvant 1 week after immunization showing vacuoles (white arrows) containing fine granular and dense material and intact cell organelles (×15 000); (c) a brain section of a juvenile mouse treated with tetanus toxoid adsorbed on alum adjuvant 1 week after immunization showing the nucleus (star) at the right, a few dense bodies, and many mitochondria that appear in shrunken form (yellow arrow). Notice the intact organelles at the lower part (white arrow) (×8000); (d) an adult mouse treated with tetanus toxoid adsorbed on calcium phosphate nanoparticles adjuvant 1 week after immunization showing large indented nucleus (star) with uniformly thick heterochromatin (white arrows), the upper and lower border of the cell surrounded with necrotic tissue debris, and some vacuoles contain dense bodies (blue arrow) and other contain pale bodies (black arrow) (×15 000); (e) a juvenile mouse immunized with tetanus toxoid adsorbed on calcium phosphate nanoparticle adjuvant 1 week after immunization shows a few mitochondria (yellow arrow), some vacuoles that contain dense bodies (blue arrow), and a large indented nucleus (star) with uniformly thick heterochromatin (white arrows) (×15 000).

Morphometric study

Effect on the liver

Morphometric study of the nucleus/cell ratio (N/C) of control liver of nonimmunized mice revealed mean value equal to 0.322 ± 0.014, whereas the damaged area recorded a value of 0.00 (Tables 1 and 2).

In the alum adjuvant group, the N/C ratio of liver sections of adult mice recorded a mean value of 0.702 ± 0.494, which showed a significant increase ($P < 0.05$), and the damaged area within the same sample recorded a mean value of 4151.50 ± 2260.81, which also showed a significant increase ($P < 0.05$) as compared with controls (Tables 1 and 2). Measurement of the N/C ratio of the liver of juvenile mice recorded a mean value of 0.424 ± 0.274, which showed a significant decrease ($P < 0.05$), whereas the damaged area within the same sample recorded a mean value of 3556.89 ± 2027.05, which also showed a significant increase as compared with controls ($P < 0.05$) (Tables 1 and 2).

In the CAP nanoparticle adjuvant group, measurement of the N/C ratio of the liver sections of adult mice recorded a mean value of 0.865 ± 0.591, which showed a significant increase ($P < 0.05$) as compared with controls, and the damaged area within the same sample recorded a mean value of 3349.21 ± 1831.01, which also showed a significant increase ($P < 0.05$) as compared with controls (Tables 1 and 2). Measurement of the N/C ratio of the liver sections of juvenile mice recorded a mean value of 0.389 ± 0.159, which showed a significant increase ($P < 0.05$), and the

Table 1 Nucleus/cell ratio area change in the liver, kidney, and brain tissues of adult and juvenile mice after 1 week of immunization with tetanus toxoid adsorbed on alum and calcium phosphate nanoparticle adjuvants

Parameters	Groups N/C ratio Liver	Kidney	Brain
Control	0.322 ± 0.014	0.678 ± 0.036	0.299 ± 0.020
Alum (adult)	0.702 ± 0.494*	0.528 ± 0.290*	0.455 ± 0.235*
Alum (juvenile)	0.424 ± 0.274*	0.652 ± 0.415	0.473 ± 0.242*
Calcium phosphate (adult)	0.865 ± 0.591*	0.671 ± 0.402	0.272 ± 0.122
Calcium phosphate (juvenile)	0.389 ± 0.159*	0.724 ± 0.747*	1.103 ± 0.893*

*Significant difference than control at $P < 0.05$.

Table 2 Damaged area in the liver tissue of adult and juvenile mice after immunization with tetanus toxoid adsorbed on alum and calcium phosphate nanoparticle adjuvants 1 week after immunization

Parameters	Groups Damaged area (μm^2) Liver
Control	0.00
Alum (adult)	4151.50 ± 2260.81*
Alum (juvenile)	3556.89 ± 2027.05*
Calcium phosphate (adult)	3349.21 ± 1831.01*
Calcium phosphate (juvenile)	2031.73 ± 706.20*

*Significant difference than control at $P < 0.05$.

damaged area within the same sample recorded a mean value of 2031.73 ± 706.20, which also showed a significant increase ($P < 0.05$) (Tables 1 and 2).

Effect on the kidney

Measurement of the N/C ratio of control kidney of nonimmunized mice recorded a mean value of 0.678 ± 0.036 (Table 1).

In the alum adjuvant group, measurement of the N/C ratio of kidney sections of adult mice revealed a mean value of 0.528 ± 0.290, which showed a significant change ($P < 0.05$), whereas juvenile mice revealed a mean value of 0.0.652 ± 0.415 (Table 1).

In the CAP nanoparticle adjuvant group, measurement of the N/C ratio of kidney sections of adult mice revealed a mean value of 0.671 ± 0.402, whereas juvenile mice revealed a mean value of 0.724 ± 0.747, which showed a significant increase as compared with controls ($P < 0.05$) (Table 1).

Effect on the brain

Measurement of the N/C ratio of control brain of nonimmunized mice revealed a mean value of 0.299 ± 0.020 (Table 1).

In the alum adjuvant group, measurement of the N/C ratio of brain sections of adult mice revealed a mean value of 0.455 ± 0.235, which showed a significant increase ($P < 0.05$) compared with controls, whereas that of juvenile mice revealed a mean value of 0.473 ± 0.242, which showed a significant increase ($P < 0.05$) compared with controls (Table 1).

In the CAP nanoparticle adjuvant group, measurement of the N/C ratio of brain sections of adult mice revealed a mean value of 0.272 ± 0.122, whereas that of juvenile mice revealed a mean value of 1.103 ± 0.893, which showed a significant increase ($P < 0.05$) as compared with controls (Table 1).

Discussion

Vaccines have profound impact on global health, although concerns persist about their potential role in autoimmune or other adverse reactions [16]. To address these concerns, vaccine components such as immunogens and adjuvants require critical evaluation for healthy individuals and their safety. In the present study, aluminum phosphate and CAP nanoparticles were prepared and used as adjuvants. The current work aimed at studying the pathological ultrastructural and morphometrical effect of both alum and CAP nanoparticle adjuvants.

The results of the electron microscopic study revealed wide and severe ultrastructural changes in the liver tissue in both the alum and CAP nanoparticle adjuvant groups, which were more obvious in adult mice in the CAP nanoparticle group and in juvenile mice in the alum group. These changes included degenerated nuclear envelope with unusual chromatin picture of nucleus, degenerated cytoplasm, altered rough endoplasmic reticulum, and swollen mitochondria with degenerative cristae.

The ultrastructural changes occurring in the kidney of both adult and juvenile mice in the alum adjuvant group included developing large vacuoles containing cell debris, shrunken nucleus with irregular outline, unusual chromatin picture of nucleus, and appearance of lymphocytes. In the CAP nanoparticle adjuvant with alum group and juvenile group, the changes included swollen mitochondria with degenerated cristae, severely degenerated ground cytoplasm, and unusual chromatin picture of nucleus.

The ultrastructural changes occurring in the brain were more obvious in adult mice when using CAP nanoparticle adjuvant and in juvenile mice when using alum adjuvant, and it included both the adult and juvenile groups in case of using alum and CAP nanoparticle adjuvant, including the appearance of vacuoles containing fine granular dense material, intact cellular organelles, and shrunken mitochondria. Mitochondrial dysfunction or disease presented a malfunction in the biochemical process of energy production, resulting from disruption of either mitochondrial DNA or nuclear DNA [17–19]. This has been studied in patients with brain diseases, including neurodegenerative diseases and, to some extent, psychiatric disorders [20–21]. In case of using calcium nanoparticles adjuvant in both the adult and juvenile groups, the changes included appearance of necrotic tissue debris and vacuoles containing dense material.

Morphometric changes in the studied liver revealed changes in N/C ratio and damaged area and showed a significant change in both the alum and CAP nanoparticle adjuvant groups in both adult and juvenile groups.

The morphometric study of the kidney showed changes in N/C ratio, which were significant when using alum adjuvant with adult mice but not significant with juvenile ones. In contrast, when using CAP nanoparticle adjuvant, the changes in N/C ratio were significant with juvenile but not significant with adult mice.

As regards the morphometric changes that occurred in the brain, the changes in N/C ratio were significant when using alum adjuvant with both adult and juvenile mice. In the CAP nanoparticle adjuvant group, the changes in N/C ratio were significant when using it in juvenile mice but not significant with adult mice.

Conclusion

Both adjuvants have pathological effect on the ultrastructures and the N/C ratio of the cell. The changes were noticed in the liver, kidney, and brain. From this study, it becomes evident that further studies are needed to minimize the pathological effects of the already used adjuvants and more studies must be directed to new potent adjuvants with less pathological effects.

Conflicts of interest

There is no conflict of interest.

REFERENCES

1 Leclerc C, Dériaud E, Rojas M, Whalen RG. The preferential induction of a Th1 immune response by DNA-based immunization is mediated by the immunostimulatory effect of plasmid DNA. Cell Immunol 1997; 17997–106.

2 Manmohan S. Vaccine adjuvants and delivery systems. Hoboken, New JerseyWiley Interscience, John Wiley & Sons Inc2007; .

3 Cox JC, Coulter AR. Adjuvants – a classification and review of their modes of action. Vaccine 1997; 15248–256.

4 Confavreux C, Suissa S, Saddier P, Bourdès V, Vukusic S. Vaccinations and the risk of relapse in multiple sclerosis. Vaccines in Multiple Sclerosis Study Group. N Engl J Med 2001; 344319–326.

5 Averhoff F, Mahoney F, Coleman P, Schatz G, Hurwitz E, Margolis H. Immunogenicity of hepatitis B Vaccines. Implications for persons at occupational risk of hepatitis B virus infection. Am J Prev Med 1998; 151–8.

6 Yuen MF, Lim WL, Cheng CC, Lam SK, Lai CL. Twelve-year follow-up of a prospective randomized trial of hepatitis B recombinant DNA yeast vaccine versus plasma-derived vaccine without booster doses in children. Hepatology 1999; 29924–927.

7 Zhang L, Gu FX, Chan JM, Wang AZ, Langer RS, Farokhzad OC. Nanoparticles in medicine: therapeutic applications and developments. Clin Pharmacol Ther 2008; 83761–769.

8 Emerich DF, Thanos CG. Targeted nanoparticle-based drug delivery and diagnosis. J Drug Target 2007; 15163–183.

9 Singh M, Carlson JR, Briones M, Ugozzoli M, Kazzaz J, Barackman J*et al.* A comparison of biodegradable microparticles and MF59 as systemic adjuvants for ecombinant gD from HSV-2. Vaccine 1998; 161822–1827.

10 Gupta RK. Aluminum compounds as vaccine adjuvants. Adv Drug Deliv Rev 1998; 32155–172.

11 Lindblad EB. Aluminium adjuvants in theory and practical applicaton of adjuvants. In: Stewart-Tull DES, eds. Chichester: John Wiley & Sons; 1995;21–35.

12 Anderson TD, Cheville NF. Ultrastructural morphometric analysis of Brucella abortus-infected trophoblasts in experimental placentitis. Bacterial replication occurs in rough endoplasmic reticulum. Am J Pathol 1986; 124226–237.

13 Anderson TD, Cheville NF, Meador VP. Pathogenesis of placentitis in the goat inoculated with Brucella abortus. II. Ultrastructural studies. Vet Pathol 1986; 23227–239.

14 Coulter HD. Rapid and improved methods fr embedding biological tissues in Epon 812 and Araldite 502. J Ultrastruct Res 1967; 20346–355.

15 Gawish AM, Issa AM, Hassan AM, Ramdan SH. Morphometrical, histopathological, and cytogenetical ameliorating effects of green tea extract on nicotine toxicity of the testis of rats. J Am Sci 2010; 6401–411.

16 Powell MF, Newman MJ. Adjuvant properties of aluminum and calcium compounds. Vaccine design: the subunit and adjuvant approach. New York, NYPlenum Publishing Corp1995; 229–248.

17 Shanske AL, Shanske S, Di Mauro S. The other human genome. Arch Pediatr Adolesc Med 2001; 1551210–1216.

18 Orth M, Schapira AH. Mitochondria and degenerative disorders. Am J Med Genet 2001; 10627–36.

19 Chinnery PF, Schon EA. Mitochondria. J Neurol Neurosurg Psychiatry 2003; 741188–1199.

20 Johns DR. The other human genome: mitochondrial DNA and disease. Nat Med 1996; 21065–1068.

21 Schon EA, Manfredi G. Neuronal degeneration and mitochondrial dysfunction. J Clin Invest 2003; 111303–312.